

Nanostructured Metal-Organic Composite Solar Cells

Investigators

Mark L. Brongersma, Assistant Professor, Materials Science and Engineering; Shanhui Fan, Assistant Professor, Electrical Engineering; Peter Peumans, Assistant Professor, Electrical Engineering; Peter Catrysse, Post-doctoral researcher; Ed Bernard and Jung-Yong Lee Graduate Researchers.

Abstract

This project aims at realizing a high efficiency organic photovoltaic device using the multijunction concept and metal nanoscale features to enhance the overall cell performance. In particular, transparent high-sheet-conductivity nanopatterned metal films are being developed for use as transparent conductors allowing parallel subcell connection, and metal nanostructures are being embedded in the active layers to enhance the photon absorption and charge separation efficiency. This year we discovered that by concentrically filling nano-scale holes in metal contacts with different dielectric materials, it is possible to significantly extend the bandwidth of an optical mode (HE_{11}) that enables efficient light transmission through the metal. We have also made significant progress in the design and optical analysis of metallic nano-antenna\field concentrating structures. A darkfield microscope was successfully constructed to determine and subsequently optimize the resonance properties of individual nanoscale antennas.

Introduction

Organic-based solar cells have high potential to reduce the cost of photovoltaics. Low-cost active materials, high-throughput reel-to-reel deposition technologies, and application versatility makes them very likely to become competitive against inorganic thin-film devices. However the power conversion efficiency of organic photovoltaics (OPV) is still too low. This project aims at realizing a high efficiency organic devices by exploiting the unique optical properties of metal to realize high-sheet-conductivity and virtually transparent contacts. It also aims at optimizing the use of metal nanostructures in the active layers to enhance the photon absorption and charge separation efficiency.

Background

The performance of organic photovoltaics has been improving relatively quickly in the last few years. However this technology is still facing major fundamental limitations towards higher efficiency and stability that need to be overcome for it to be competitive with inorganic thin-film solar cells. This project proposes an innovative cell design to increase the efficiency of organic photovoltaics: a stack of organic/inorganic heterojunctions with embedded nanostructured metal features to improve the overall cell performance. The stack design is a high potential route to increase the light absorption efficiency of photovoltaics. The splitting of the solar spectrum through complementary absorption by different cells with specifically designed bandgaps minimizes thermal losses and increases the overall photon conversion efficiency.

Results

During the last year, progress has been made three different research directions outlined below. Two new approaches for transparent contacts were investigated and advances were made in the synthesis and characterization of metallic antenna structures.

First, we describe our most recent results pertaining to developing nanoengineered transparent metal contacts. The replacement of transparent metal oxides such as indium-tin-oxide (ITO), by a cheaper and higher performance alternative is important for many thin-film photovoltaic cells. Metal oxides have a number of disadvantages. The cost of sputtered ITO thin films may be too high for applications in solar cells and large-area light-emitting diodes (LEDs) for lighting. Moreover, the cost of ITO is likely to increase further due to the potential shortage of indium. On flexible substrates, the brittleness of metal oxides leads to film cracking under bending, ultimately leading to device failure. In cases where a transparent electrode is required on top of an organic layer, the sputter deposition of ITO onto an organic material is known to cause damage to the underlying organic layers that leads to decrease in device performance. Lastly, there is an inherent trade-off between optical transparency and sheet resistance. Thicker films and a high doping concentration increases the film conductivity, but also decreases the optical transparency, as shown in Fig. 1. For a sheet resistance of $R_{sh}=10\Omega/sq$, the solar photon flux-weighted optical transparency is $T_{SW}<80\%$.

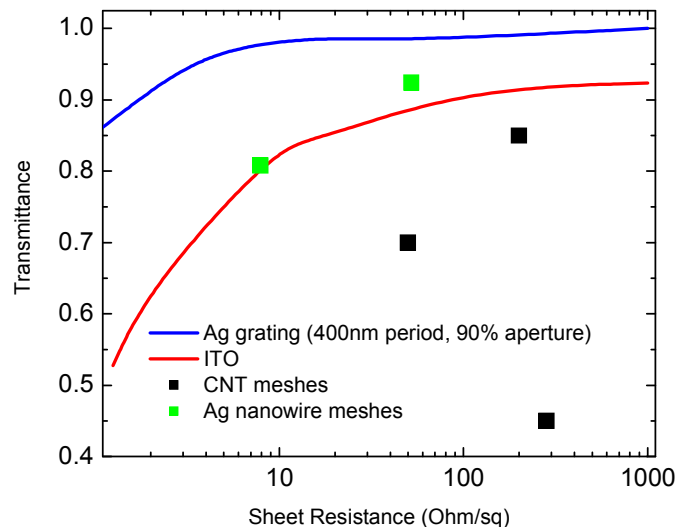


Figure. 1: Comparison of the performance of ITO (red line) as a transparent electrode to alternatives. The transmission is plotted vs the sheet resistance. A good transparent electrode has a high transmittance ($>90\%$) and a low sheet resistance ($<10\Omega/sq$). Carbon nanotube meshes (black markers) are not attractive compared to ITO at this time. Periodic metal nanowire gratings (blue line) are very attractive and outperform ITO. As a low-cost alternative, meshes of Ag nanowires, that can be processed from solution, outperform ITO as well.

We have investigated the use nanostructured metal electrodes as transparent conducting electrodes. Using modeling, we have shown that the optical transmission and sheet resistance of subwavelength metal gratings is superior to that of ITO. For a sheet

resistance $>5\Omega/\text{sq}$, the optical transmissivity is $>95\%$ for a large part of the solar spectrum. Finite-element modeling was used to calculate the optical transmittance of subwavelength metal gratings as a function of the geometric parameters of the gratings. In Fig. 2a, the optical electric field (contours) and Poynting vector (arrows) are shown for a TE and TM mode incident on an Ag grating with a period of 400nm and a metal linewidth of 40nm (geometric aperture of 90%). The optical transmittance is shown for the TE and TM polarization in Fig. 2b. The solar spectrum is shown for comparison. The observation that the transmission can be as high as 99% for a certain part of the solar spectrum, indicates that metal gratings are not only transparent, but they also index match to the surrounding medium (in this case vacuum).

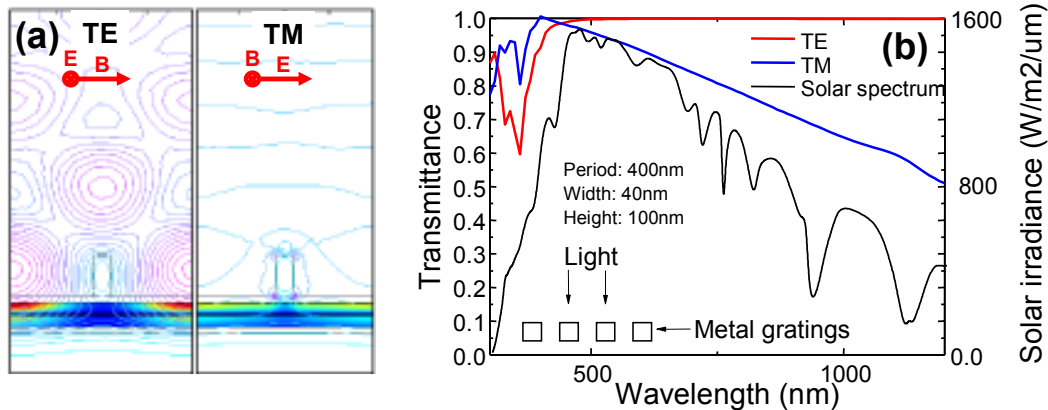


Figure 2: (a) Finite element modeling of transmission through metal gratings. The contours are for the magnitude of the electric field. The colored regions indicate the power absorbed per unit volume in an underlying organic solar cell structure. (b) Transmission of the TE and TM mode of a metal grating. The solar spectrum is shown for comparison. The metal grating is transparent to most of the solar spectral photons.

As an alternative to metal subwavelength gratings that may be hard and expensive to fabricated, we have shown that random meshes of metal nanowires processed from solution achieve a performance that approaches that of the periodic metal gratings. A solar photon flux averaged transmissivity of $T_{\text{SW}} = 80\%$ for a sheet resistance of $R_{\text{sh}}=40\Omega/\square$ was achieved for such a solution processed transparent thin-film electrode (see Fig. 1). In Fig. 3a, electron microscope images of a metal nanowire mesh electrode are shown. As deposited, the sheet resistance is high due to a polymer coating that is used during the synthesis. Upon annealing at 200°C for 20 minutes, the sheet resistance drops drastically and the resulting films are now an improvement over ITO at a small fraction of the cost and thermal budget.

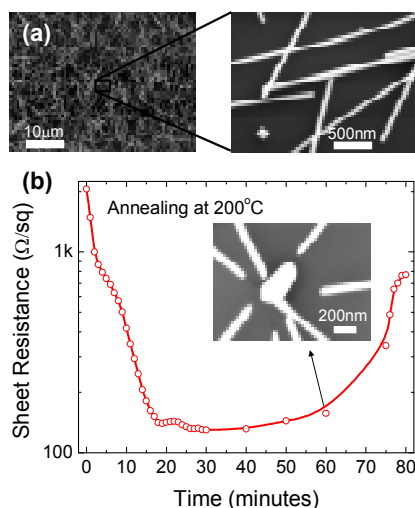


Fig. 3. (a) Scanning electron micrographs of Ag nanowire meshes deposited by drop casting. (b) Sheet resistance of an Ag nanowire mesh as deposited upon annealing at 200°C.

We fabricated organic photovoltaic cells on transparent metal nanowire mesh electrodes and have shown that cells on metal nanowire meshes exhibit improved photocurrents compared to identical cells that use ITO for the transparent electrode, as shown in Fig. 4.

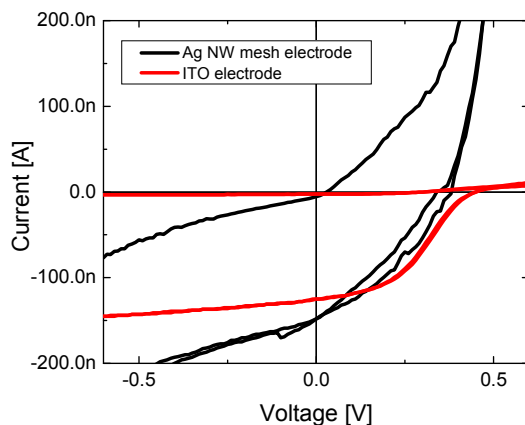


Fig. 4. Comparison of the performance of an organic solar cell on a metal nanowire mesh (black lines) to that of a cell on conventional ITO (red lines).

We have also investigated the possibility to make metal contacts transparent by introducing deep-subwavelength holes into them. For sub-wavelength apertures in metallic films, it is well known that the transmission characteristics are strongly influenced by the presence or absence of propagating optical modes inside the apertures. For cylindrical holes with a circular cross section, the prevailing wisdom dictates that they do not support propagating modes when the hole diameter is much smaller than $\lambda/2n_0$, where λ is the vacuum wavelength of incident light and n_0 is the refractive

index of the dielectric filling the hole. Nevertheless, sub-wavelength cylindrical holes in a plasmonic metal, in fact, always support a propagating mode near the surface plasmon frequency, regardless of how small the holes are. The propagating HE_{11} mode is located completely below the surface plasmon frequency and gives rise to a pass-band in the transmission spectrum. However, the bandwidth of the HE_{11} mode asymptotically approaches zero as hole size is reduced to zero. Thus such a mode may not play a prominent role as the hole size becomes far smaller than the wavelength of the incident light.

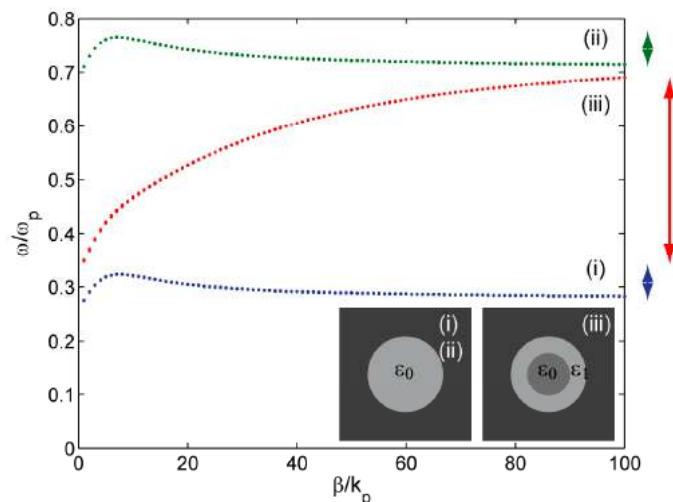


Figure 5: Propagating HE_{11} mode of a nano-scale hole in metal with plasma wavelength λ_p . (e.g. or silver $\lambda_p = 138\text{nm}$). Dispersion diagram for (i) low-index core (Green curve, $r_0 = 0.036$, $\lambda_p = 5\text{nm}$, $\epsilon_0 = 1$). (ii) High index core. (Blue curve, $r_0 = 0.036$, $\lambda_p = 5\text{nm}$, $\epsilon_0 = 12$). (iii) Dielectric core with concentric rings of high and low indices. (Red curve.)

With the support of the GCEP program, we very recently discovered that by concentrically filling nano-scale holes with two different dielectric materials, it is possible to significantly extend the bandwidth of the HE_{11} mode. By dispersion relation analysis, we show that using this approach it is possible to create nano-scale propagating modes with very large bandwidth even when the hole radius goes to zero. (Figure 5)

The structure we consider is shown in the inset (iii) of Fig. 5 and represents a z -invariant waveguide with a cylindrical cross-section in the transverse xy -plane with an external radius r_m . Inside the waveguide, we assume two concentric dielectric regions: a central disk with radius r_1 and a concentric ring of width $r_m - r_1$. For the dielectric materials inside these regions, we use real frequency-independent dielectric constants ϵ_1 and ϵ_2 . For the surrounding metal, we use a complex frequency-dependent model:

$$\epsilon_m(\omega) = 1 - \frac{\omega_p^2}{\omega(\omega - i\omega_\tau)}, \quad (1)$$

where ω_p is the plasma frequency and ω_τ is the collision frequency. We derive and solve a transcendental equation to calculate the dispersion relation (β, ω) of propagating modes inside a cylindrical hole, where β is the propagation vector along the z -axis of the waveguide and ω is the radial frequency.

In general, sub-wavelength holes in a plasmonic metal always support a fundamental HE_{11} mode that is spectrally defined between an upper and a lower frequency limit. The upper limit occurs for $\beta \rightarrow \infty$ and asymptotically approaches the surface plasmon frequency $\omega_{sp} = \omega_p / \sqrt{\epsilon_0 + 1}$ of the metal-dielectric interface inside the hole, where ϵ_0 is the dielectric constant of the dielectric near the interface. In this limit, the mode is tightly confined to the metal-dielectric interface and senses the dielectric and metal in its immediate vicinity only. The lower limit occurs when $\beta = 0$ and represents the cutoff frequency ω_c of the HE_{11} mode. For holes filled with a uniform dielectric, the limiting frequencies are intrinsically coupled through the dielectric constant of the uniform material inside the hole. As a result, the cutoff frequency ω_c of the HE_{11} mode asymptotically approaches surface plasmon frequency ω_{sp} and the bandwidth of the mode, $\omega_{sp} - \omega_c$ goes to zero when hole size is reduced to deep sub-wavelength scale, which is required for many transparent electrode applications.

The observation that ω_{sp} depends on the dielectric properties in the immediate vicinity of the interface only, while ω_c depends on the dielectric properties across the entire hole, however, provides a possible mechanism for decoupling the limiting frequencies of the HE_{11} mode through the use of concentric dielectric rings. By effectively decoupling the dependence of the cut-off frequency ($\beta = 0$) from that of the large- β frequency, it is possible to engineer the behavior of both frequency limits (for $\beta = 0$ and $\beta \rightarrow \infty$) independently. This in turn enables complete control over the mode bandwidth. We note that in order to extend bandwidth, the cut-off frequency has to be lowered and the upper-frequency limit has to be raised. This is achieved by appropriate choice of dielectrics, i.e., the center region has to have a larger index and the concentric ring a lower index. (Figure 5)

Figure 6 shows a vector plot of the electric (displacement) field for the fundamental HE_{11} mode in a sub-wavelength hole filled with two concentric dielectric regions. The field orientation provides evidence that the propagating mode indeed has the proper symmetry for efficient coupling. Similarly, we have examined the fields of the next-higher-order EH_{11} mode (not shown here) and confirmed that it couples to normally incident light as well. This field analysis confirms the usefulness of these propagating modes in transporting of light collected/emitted at the entrance/exit of a sub-wavelength aperture.

In order to increase current generation in the active layer of an organic solar cell, we have also synthesized metallic nanowire structures by electrochemical means into porous materials, such as nanoporous anodized alumina or ion track-etched polycarbonate (PC) membranes. By embedding such structures in OPV devices an improved light absorption, charge separation, and charge collection can be obtained. For example, when placed at the donor-acceptor interface of an organic heterojunction, electrically isolated metal nanoparticles may enhance photon absorption by concentrating the electromagnetic energy of incident radiation close to the junction.

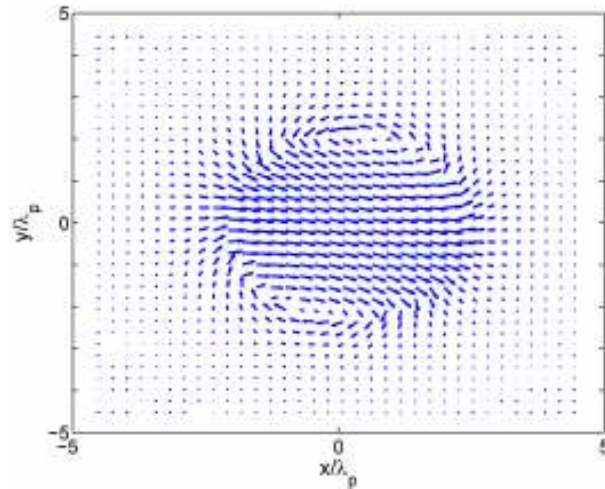


Figure 6: Electric field distributions for the propagating HE_{11} mode in a subwavelength cylindrical hole in metal. The dipolar field indicates that the mode will couple to external plane waves.

We have also successfully constructed a dark-field optical microscope to study the wires in real space and to take scattering spectra of individual wires. To investigate our nanowire growth process and the operation of the microscope, we generated calibration samples consisting of hybrid wires with Au and Ag sections. Fig. 7(a) shows a scanning electron microscopy image of such a hybrid wire.

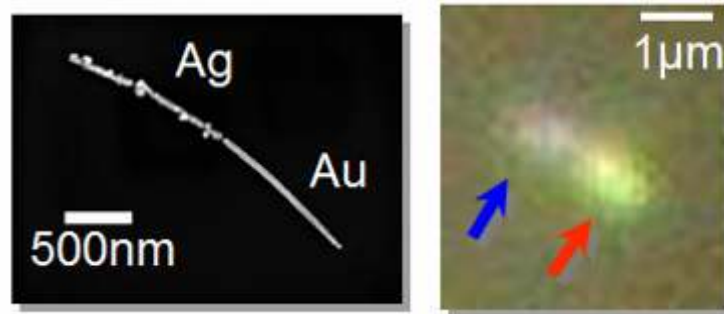


Figure 7: (a) Scanning electron microscopy (SEM) image of a hybrid Ag/Au nanowire generated by electroplating of Ag and Au into a porous polycarbonate membrane (b) Dark-field optical microscopy image of the same wire. The blue and red arrows indicate the location of the Ag and Au sections of the wire.

Figure 7(b) is a darkfield microscopy image of the same wire that clearly shows the different lightscattering properties of the two metals. We were also able to take darkfield scattering spectra from the different sections of the wire and compare them to light scattering (Mie) theory. Figure 8(a) and (c) show the measured lightscattering spectra from the Ag and Au segments respectively. The good agreement with Mie theory presented in figures 8(b) and (d), enabled us to start systematic investigations of the lightscattering from wires of different diameter and length.

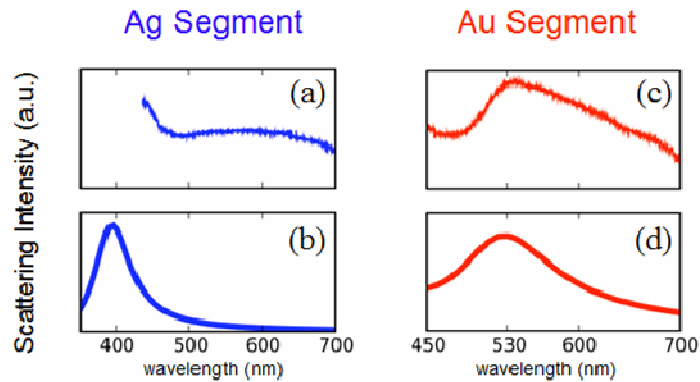


Figure 8: Measured (a and c) and simulated lightscattering spectra (b and d) from the Au (in blue) and Ag (in red) segments of the hybrid nanowire shown in Fig. 7(a).

Progress

If successful, transparent metal contacts and antennas will significantly enhance solar cell performance and offer increased competitiveness of OPV for clean energy production compared to routes that ultimately lead to green house gas emissions. In order to have a global impact, methods for efficient scaling of this technology will have to be explored in a second phase.

Future Plans

We will continue our efforts to generate transparent metal contacts. Improved metal nanowire meshes will be investigated and the mechanism for the enhancement in solar cell performance observed in Fig. 4 will be explored using near-field optical microscopy as well as confocal microscopy. Based upon the recent results on engineered nanoscale apertures, we will now specifically design plasmonic thin film structures in which the propagating bandwidths are greatly enlarged. A systematic study of the resonant properties of nanowire antenna was initiated and the best antennas will be incorporated into OPV cells.

Publications

1. P. B. Catrysse and S. Fan, "Near-complete transmission through sub-wavelength hole arrays in phonon-polariton thin films", *Physical Review B* 75, 075422 (2007).
2. Ed Barnard and Mark L Brongersma, "Metallic Nanowire Optical Antennas", Materials Research Society Fall Meeting, Boston, 2005

Contacts

Brongersma@stanford.edu, Ppeumans@stanford.edu, Shanhui@stanford.edu